International Journal of Nanomedicine

Dovepress

open access to scientific and medical research

Open Access Full Text Article

ORIGINAL RESEARCH

Cuprous oxide nanoparticles reduces hypertrophic scarring by inducing fibroblast apoptosis

This article was published in the following Dove Press journal:
International Journal of Nanomedicine

Yongqiang Xiao[1,*]
Dayuan Xu[1,*]
Hongyuan Song[2,*]
Futing Shu[1]
Pei Wei[3]
Xiaolan Yang[3]
Chenjian Zhong[3]
Xiaohong Wang[4]
Werner EG Müller[4]
YongJun Zheng[1]
Shichu Xiao[1,*]
Zhaofan Xia[1]

[1]Department of Burn Surgery, Changhai Hospital, Second Military Medical University, Shanghai, People's Republic of China; [2]Department of Ophthalmology, Changhai Hospital, Second Military Medical University, Shanghai 200433, People's Republic of China; [3]Department of Burns Surgery, Union Hospital, Fujian Medical University, Fuzhou 350001, People's Republic of China; [4]Erc Advanced Investigator Grant Research Group at the Institute for Physiological Chemistry, University Medical Center of the Johannes Gutenberg University, Mainz 55128, Germany

*These authors contributed equally to this work

Correspondence: Zhaofan Xia; Yongjun Zheng
Department of Burn Surgery, Changhai Hospital, Second Military Medical University, 168 Changhai Road, Shanghai, People's Republic of China
Tel +86 213 116 1821; +86 213 116 1828
Fax +86 216 558 9829; +86 216 558 9829
Email xiazhaofan_smmu@163.com; smmuzhengyongjun@163.com

Background: Less apoptosis and excessive growth of fibroblasts contribute to the progression of hypertrophic scar formation. Cuprous oxide nanoparticles (CONPs) could have not only inhibited tumor by inducing apoptosis and inhibiting proliferation of tumor cells, but also promoted wound healing. The objective of this study was to further explore the therapeutic effects of CONPs on hypertrophic scar formation in vivo and in vitro.

Methods: In vivo, a rabbit ear scar model was established on New Zealand albino rabbits. Six full-thickness and circular wounds (10 mm diameter) were made to each ear. Following complete re-epithelization observed on postoperative day 14, an intralesional injection of CONPs or 5% glucose solution was conducted to the wounds. The photo and ultrasonography of each wound were taken every week and scars were harvested on day 35 for further histomorphometric analysis. In vitro, the role of CONPs in human hypertrophic scar fibroblasts (HSFs) apoptosis and proliferation were evaluated by Tunnel assay, Annexin V/PI staining, cell cycle analysis, and EdU proliferation assay. The endocytosis of CONPs by fibroblasts were detected through transmission electron microscopy (TEM) and the mitochondrial membrane potential and ROS production were also detected.

Results: In vivo, intralesional injections of CONPs could significantly improve the scar appearance and collagen arrangement, and decreased scar elevation index (SEI). In vitro, CONPs could prominently inhibit proliferation and induce apoptosis in HSFs in a concentration-dependent manner. In addition, CONPs could be endocytosed into mitochondria, damage the mitochondrial membrane potential and increase ROS production.

Conclusion: CONPs possessed the therapeutic potential in the treatment of hypertrophic scar by inhibiting HSFs proliferation and inducing HSFs apoptosis.

Keywords: CONPs, hypertrophic scar, apoptosis, proliferation, mitochondria

Introduction

Hypertrophic scar is a severe fibrotic skin disease with excessive extracellular matrix deposition and abnormal remodeling after cutaneous wounds involved in dermal tissue.[1,2] Scarring that manifested severe sequelae such as persistent itching and pain, organ dysfunction or body disfiguration, often lead to severe physiological and psychological burden for patients and families.[3,4] Although many different kinds of prevention and treatment strategies already exist, such as excision, compression, and laser,[5,6] it is still difficult to be cured by there conventional therapy.[7] The specific mechanism underlying the hypertrophic scar formation still need be further explored. However, less apoptosis and excessive growth of fibroblasts have

been verified to play important roles in the hypertrophic scar formation.[8,9] The idea that inducing HSFs apoptosis and inhibiting HSFs proliferation could be an effective strategy for anti-hypertrophic scar therapy.[10,11] Recently, CONPs have been widely used in many anti-tumor therapies and showed great anti-tumor characteristics, such as inducing tumor cells apoptosis and inhibiting proliferation.[12,13] Moreover, CONPs have also showed potential property of promoting wound healing through inhibiting pathogenic strains, increasing blood vessel formation and some other mechanisms.[14,15] However, whether CONPs possess the potential anti-scar properties remain an undeveloped area.

Therefore, the purpose of this study was to explore the therapeutic effects of CONPs on hypertrophic scar formation in vivo and in vitro. In vivo, we discovered that CONPs could significantly improve the scar appearance and decrease SEI in a rabbit ear hypertrophic scar model. In vitro, CONPs could significantly inhibit proliferation and induce apoptosis in HSFs. Furthermore, the findings also revealed that CONPs could specifically target the mitochondria and induce apoptosis by initiating a mitochondrion-mediated apoptosis signaling pathway. Our results strongly suggest that CONPs could ultimately be applied to the treatment of hypertrophic scar as a new type of anti-scarring nanomedicine.

Methods

Synthesis and characterization detection of CONPs

CONPs were produced as described in the previous study.[16] Chemicals of analytical grade were used in the experiment. First, a total of 0.35 mL of 0.1 M CuSO4 (aq) and 3 mL of 0.1 M cetyltrimethylammonium bromide (CTAB) (aq) were added into a test tube, and then shaken vigorously by a vortex mixer for about 5 mins. Then 10 mL of fresh, cold 0.04 M NaBH4 (aq) was added into mixture. The mixture was then incubated at 26 °C–28 °C for about 18 hrs until it became bright yellow. Then the mixture was centrifuged at 12,000 rpm for 15–20 mins, and washed with ethanol and deionized water. The supernatant was discarded and the solids were vacuum-dried for 15 mins. Finally, the dried black powder was collected and stored in 4 °C.[17] The dried CONPs were diluted to 30 mg/mL in doubly distilled water for further characteristic analysis. A Malvern Instrument (Malvern Nano-ZS) was used to measure the particle size and zeta potential of CONPs. The morphology of CONPs was detected under a transmission electron microscope (TEM) (H-7650, Hitachi, Japan).

Rabbit ear hypertrophic scar model establishment

All animal studies were performed adhering to the NIH guidelines for care and use of laboratory animals and with the approval of the Animal Experiment Centre of the Second Military Medical University. The rabbit ear hypertrophic scar model was produced as described previously.[18] Briefly, 8 adult New Zealand albino rabbits (male, aged 3 months, each weighing 2.5–3 kg) were given anesthesia with 1% (10 mg/mL) pentobarbital sodium (1 mg/kg). Specifically, six full-thickness and circular wounds (10 mm diameter) were made to the bare cartilage on the ventral surface of each ear under sterile conditions. The epidermis, dermis, and perichondrium were carefully removed using a surgical blade. Next day, the wounds were sterilized again and the secretions were cleaned.

Intralesional injection

On postoperative day 14 and 21, after complete re-epithelialization, for each rabbit, an intralesional injection of CONPs were conducted to the 6 wounds of left ear and 5% glucose solution at the same volume as the CONPs were injected to the 6 wounds of right ear. Briefly, a 5% glucose solution was used to dissolve the CONPs by an ultrasonic mixer (Bilon, Shanghai, China). 0.1 mL of CONPs solution at a concentration of 1mg/ml was carefully injected into the center of each lesion from the edge of the wound with a 29-G needle. Wounds in the right ear were injected in the same way with an equal volume of 0.1 mL 5% glucose solution.

Scar evaluation and histologic analysis

The gross appearance of each wounds was observed by taking photos every week and thickness of scar was calculated using an ultrasound machine (MyLabOne, Esaote, Italy). On day 35, the scar specimens were collected for the further histological analysis. Briefly, the specimens were first fixed in 4% formaldehyde solution for 24 hrs, embedded in paraffin, cut into 5mm sections, and then stained with masson trichrome staining.

Cell culturing and EdU proliferation assay

The Ethics Committees of Changhai Hospital of the Second Military Medical University approved this study involving relevant human material, and informed consent was provided

from each participant or their family member, in accordance with the Declaration of Helsinki. HSFs were isolated from human hypertrophic scars tissue and cultured in a Dulbecco's Modified Eagle Media (DMEM) supplemented with 10% FBS, and 1% penicillin and streptomycin. All the cell experiments were performed before the fourth generation. HSFs in exponential phase were seeded and treated with different concentrations of CONPs (0, 1.25, 2.5, 5 μg/ml) for 24 hr. The macroscopic morphology was detected using a digital microscope system (IX81, Olympus, Tokyo, Japan). The HSFs were treated with the CONPs for 24 hr and then the proliferation was detected by EdU assay following the manufacturer's instructions. The images were then taken using a digital microscope system (IX81, Olympus, Tokyo, Japan).

Terminal deoxynucleotidyl transferase (TdT)-mediated dUTP nick end labeling (TUNEL) assay

To identify apoptotic cells, TUNEL staining was performed using an apoptosis detection kit (Roche, California, USA) following the manufacturer's instructions. Briefly, cells were first fixed with 4% paraformaldehyde for 30 min at room temperature, washed twice with PBS and then permeabilized with 0.1% TritonX-100. The cells were then fixed in 20 μg/mL protease K for 20 min, washed twice with PBS, and stained in sequence with TUNEL reaction mixture, converter-POD and DAPI Subtrate. The images were then taken under the fluorescence microscope (Olympus, Tokyo, Japan). Experiments were performed in 96-well plates with three biological repeat.

Annexin V/PI staining

HSFs were seeded and treated with CONP medium (0, 1.25, 2.5 and 5.0 μg/mL) in 6-well culture plates for 24 hrs. Apoptotic and necrotic cells were analyzed by using an Annexin V FITC/Propidium Iodine (PI) Apoptosis Detection Kit (BD Biosciences, San Jose, CA) following the manufacturer's instructions. Briefly, a total of 5 μL FITC-Annexin V and 10 μL PI were added to the cell suspension and incubated for 30 mins at room temperature in the dark. Cells were then analyzed using Flow Cytometer (Beckman, Los Angeles, CA, USA). The percentage of apoptotic and necrotic cells was detected.

Cell cycle assay

Before analysis, HSFs were treated with different concentrations of CONPs (0, 1.25, 2.5 and 5.0 μg/mL) for 24 hr. Then cells were harvested using 0.25% trypsin with 1mM of EDTA solution, washed twice using 2 mL 4 °C phosphate-buffered saline (PBS), resuspended in 1 mL DNA staining solution, added 10 μL permeabilization solution, and then incubated for 30 mins at room temperature in the dark. The samples were subsequently analyzed using a flow cytometer (Beckman, Los Angeles, CA, USA).

Mitochondrial membrane potential

JC-1 mitochondrial membrane Potential Assay Kit (C2006, Beyotime Biotechnology, Shanghai, China) was used to detect mitochondrial membrane potential change by flow cytometry. Before analysis, HSFs were treated with different concentrations of CONPs for 24h. Cells were then incubated with JC-1 staining for 20 min, washed with staining buffer, and detected by flow cytometry (Beckman, Los Angeles, CA, USA). The experiment was independently repeated three times. The mean fluorescence intensity in HSFs reflected the level of mitochondrial membrane potential.

Transmission electron microscopy (TEM)

Before analysis, HSFs were treated with different concentrations of CONPs for 24h. Then cells were harvested, fixed with formaldehyde and dehydrated with increasing concentrations of ethanol. Finally, cells were stained in uranylacetate, embedded in Epon, and then observed with transmission electron microscope (Hitachi, Tokyo, Japan).

Intracellular reactive oxygen species (ROS) generation

Dichlorodihydrofluorescein Diacetate (DCFH-DA) Cellular Reactive Oxygen Species Detection Assay Kit (Beyotime Institute of Biotechnology, Inc. 786O, A498) was used to detect the production of intracellular ROS levels of HSFs. HSFs were treated with an increasing concentration of CONPs for 24 h. Then the cells were collected, washed with PBS, and stained with 10 mM DCFH-DA at 37 °C for 30 min. Then the DCF fluorescence was analyzed with flow cytometer (Beckman, Los Angeles, CA, USA). The experiments are independently repeated three biological times.

Statistical analysis

SPSS 22.0 software (IBM Corporation, Armonk, NY, USA) and GraphPad Prism 6.0 (La Jolla, CA, USA) were used for statistical analysis and graphical presentations. The data were shown as mean ± standard deviation (SD). One-way ANOVA was used to analysis the data. $p<0.05$ was considered to be statistically significant.

Results

Characteristics of CONPs

TEM was used to detect the morphology of CONPs. As showed in Figure 1C, CONPs were spherical and homogeneous in the suspensions. Furthermore, the zeta potential spectrum of CONPs was shown in Figure 1A; CONPs possessed a zeta potential of 17.3±4.57 mV. The particle size distribution spectrum of CONPs was shown in Figure 1B. The CONPs had a narrow particle size distribution with a mean particle size of 88.5nm. The above characterization of the CONPs suggested that the CONPs used in our experiment possessed good quality.

CONPs reduced hypertrophic scar formation

Gross examination

On postoperative day 14, all the wounds represented total re-epithelialization. Stiff and visibly raised scars gradually formed in all the wounds. By contrast, on postoperative day 35, CONPs-treated scars improved significantly on the gross examination and became softer and less visible compared with the control group, which gradually became raised, red, and stiff after re-epithelialization (Figure 2).

Masson trichrome staining

The collagen deposition after treated with CONPs was observed by Masson trichrome staining. On postoperative day 35, the deposition of collagen was eased and the collagen fibers were well arranged in the CONPs-treated scars (Figure 3C, D), while the dense, and irregularly arranged collagens were observed in 5% glucose solution-treated scars (Figure 3A, B).

Ultrasonography and calculated SEI

Ultrasonography was used to detect the accurate thickness of scars tissue from the epithelium to cartilage and the SEI were calculated. The results showed a thinner thickness and an evident lower SEI in CONPs-treated scars than their internal controls (Figure 4).

CONPs inhibited HSFs growth and induced cell cycle arrest at G2/M phases

Gross examination

The gross examination images were taken to detect the influence of CONPs on the morphology of HSFs. As shown in Figure 5, the results of gross examination images showed that CONPs caused an evident morphology change of HSFs. Cells treated with CONPs grew slow, floating with a spherical shape, while cells in 5% glucose solution treated group were spindle and grew quick.

EdU staining

EdU proliferation assay was performed to detect the influence of CONPs on the proliferation of HSFs. After treated

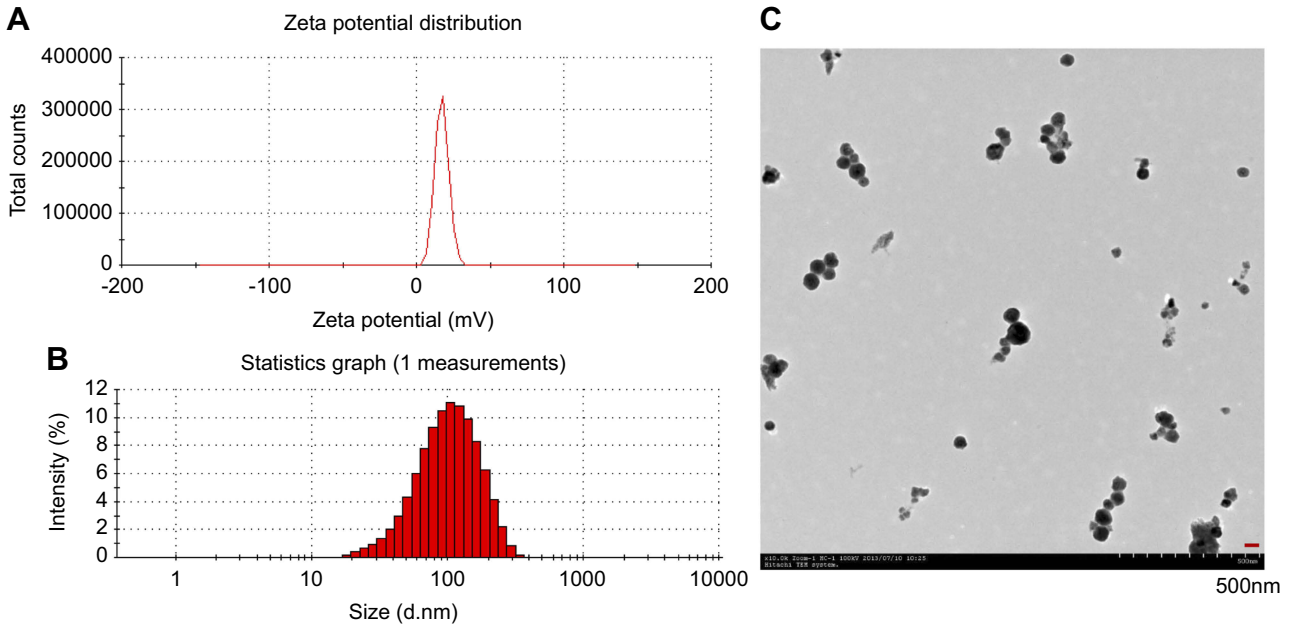

Figure 1 Characterization of the cuprous oxide nanoparticles (CONPs). (**A**) The zeta potential spectrum of CONPs; (**B**) the size distribution spectrum of CONPs; (**C**) the TEM image.

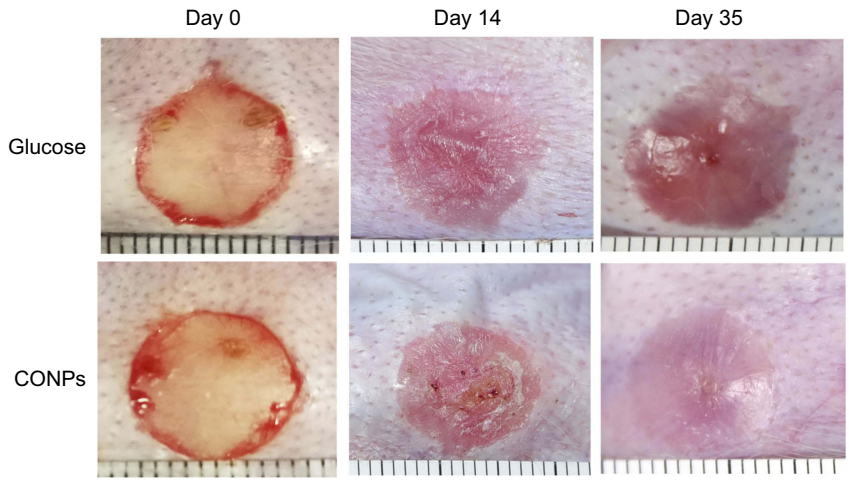

Figure 2 Gross examination images. Cuprous oxide nanoparticles (CONPs)-treated scars improved significantly on gross examination and were softer and less visible compared with their controls group, which gradually became raised, red, and stiff after re-epithelization.

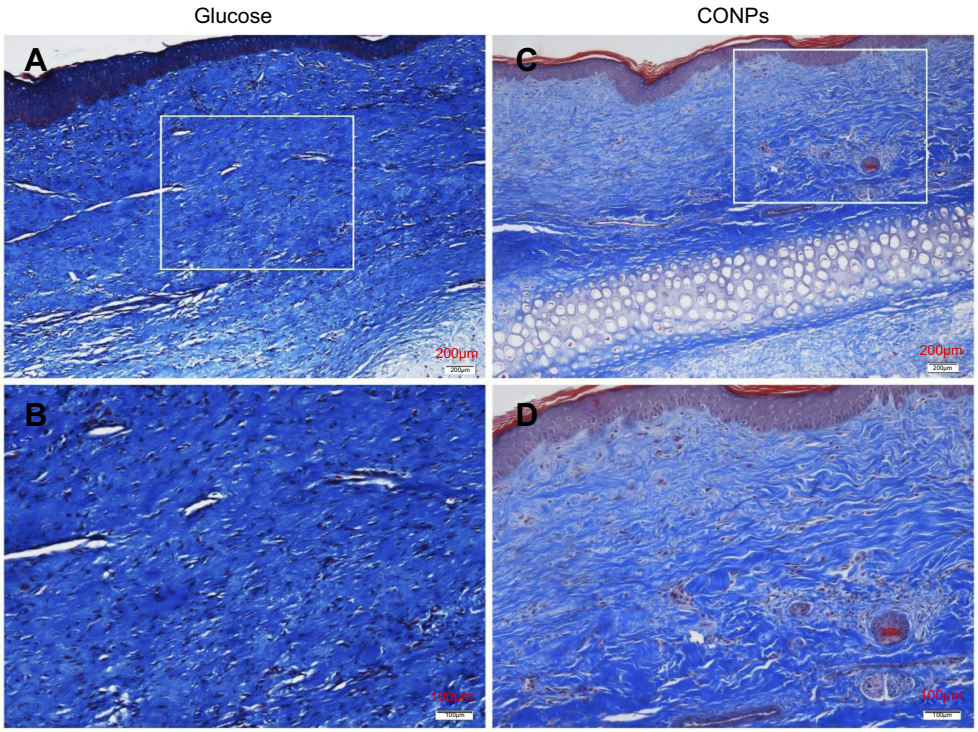

Figure 3 Masson trichrome staining. Masson trichrome staining was used for the evaluation of collagen fiber organization. Collagen fibers were dense and disorderly in the control scars (**A, B**), and significantly improved in cuprous oxide nanoparticles (CONPs)-treated scars (**C, D**).

with different concentrations of CONPs for 24 hrs, the results of EdU staining showed that the percentage of EdU positive cells was reduced gradually with the increasing concentration of CONPs, which indicated that the number of proliferating cells decreased significantly (Figure 6). All these data suggested that CONPs could suppress HSFs growth in vitro in a concentration dependent manner.

Cell cycle assay

Furthermore, the effect of CONPs on the cell cycle of HSFs was also detected by flow cytometry. As shown in Figure 7, with the increasing concentration of CONPs, the percentage of cells in G2/M phase significantly increased, while the percentage of cells in GO/G1 phase notably decreased, yet the percentage of cells

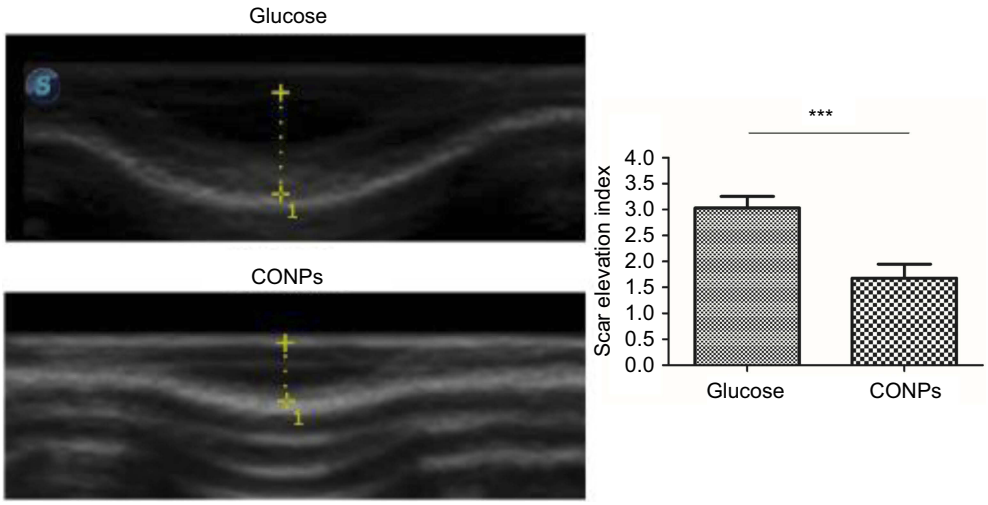

Figure 4 Ultrasonography of the wounds. The results showed a thinner thickness and an evident lower scar elevation index (SEI) in cuprous oxide nanoparticles (CONPs)-treated scars than internal controls. Column shows the quantitative measurements of the SEI of two groups. Student *t*-test was used to analyze data (***$P<0.001$).

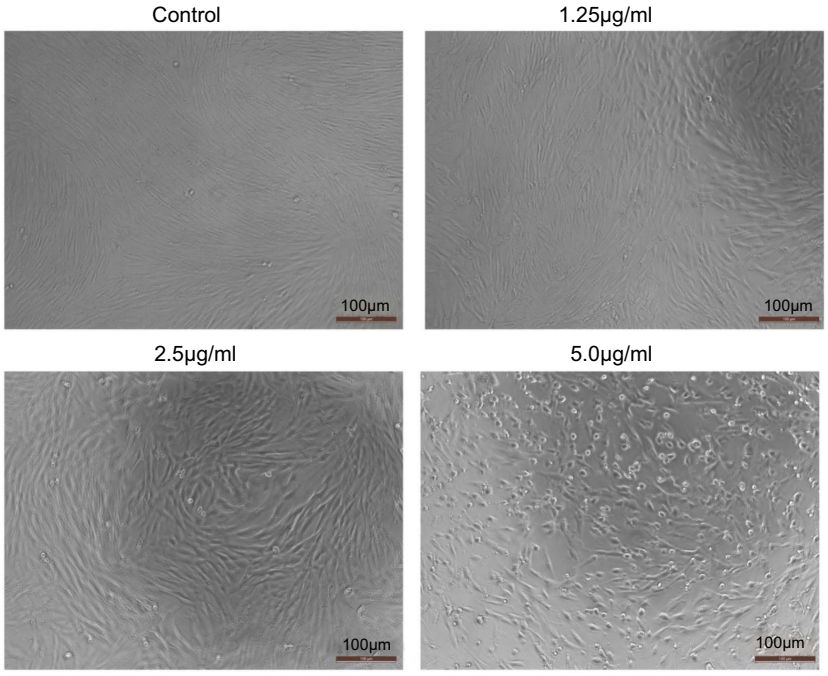

Figure 5 Effects of cuprous oxide nanoparticles (CONPs) on HSFs. The proliferation of HSFs was significantly inhibited after treated with different concentrations of CONPs. Cells treated with CONPs grew slow, floating with a spherical shape, while cells in control group were spindle and grew quick.

in S phase had no significant change. Totally, CONPs caused a significant cell cycle arrest in G2/M phase.

CONPs induced apoptosis of HSFs

To measure whether CONPs could induce the apoptosis of HSFs, Annexin V and PI-based flow cytometry analysis and TUNEL staining were performed. First of all, TUNEL staining was conducted to detect whether cell apoptosis could cause morphological changes of CONPs treated cells. As shown in Figure 8, 2.5 μg/mL and 5.0 μg/mL CONPs caused significant TUNEL positive cells in HSFs, although some weak cells after treated with CONPs were washed away during the experiment.

As shown in Figure 9, the results of flow cytometry demonstrated that HSFs treated with various concentrations

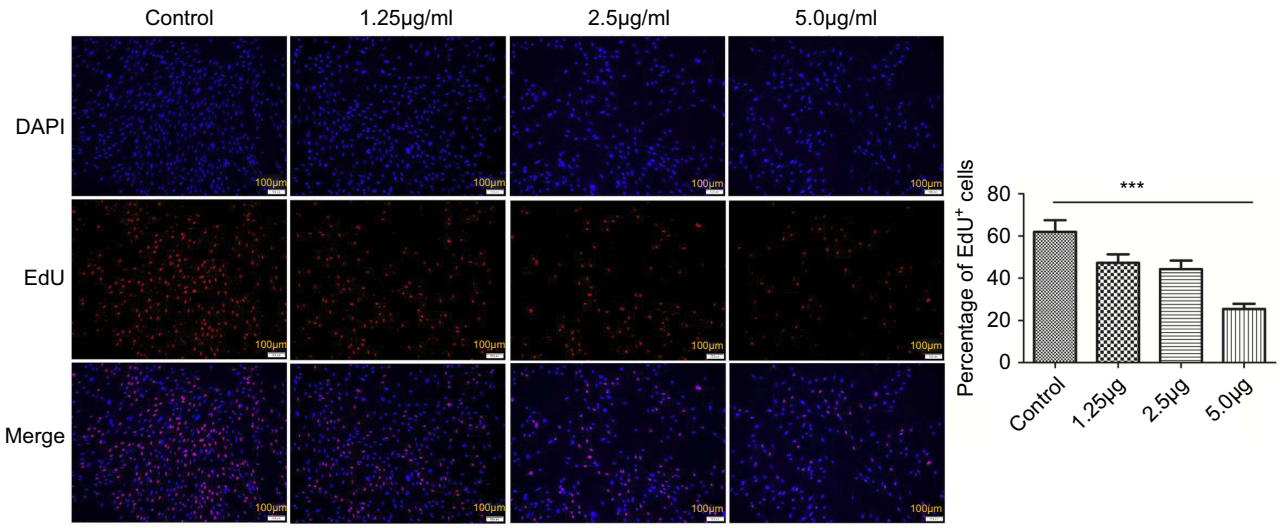

Figure 6 EdU stain of HSFs treated with different concentrations of cuprous oxide nanoparticles (CONPs) for 24h. The percentage of EdU positive cells was reduced gradually with the increasing concentration of CONPs, The proliferation of HSFs was significantly suppressed by CONPs in a dose-dependent manner. The quantitative measurements of the percentage of EdU positive cells were presented in column shows. Values are mean ± SD of three independent experiments. Significant difference is observed and compared with each group (***P<0.001).

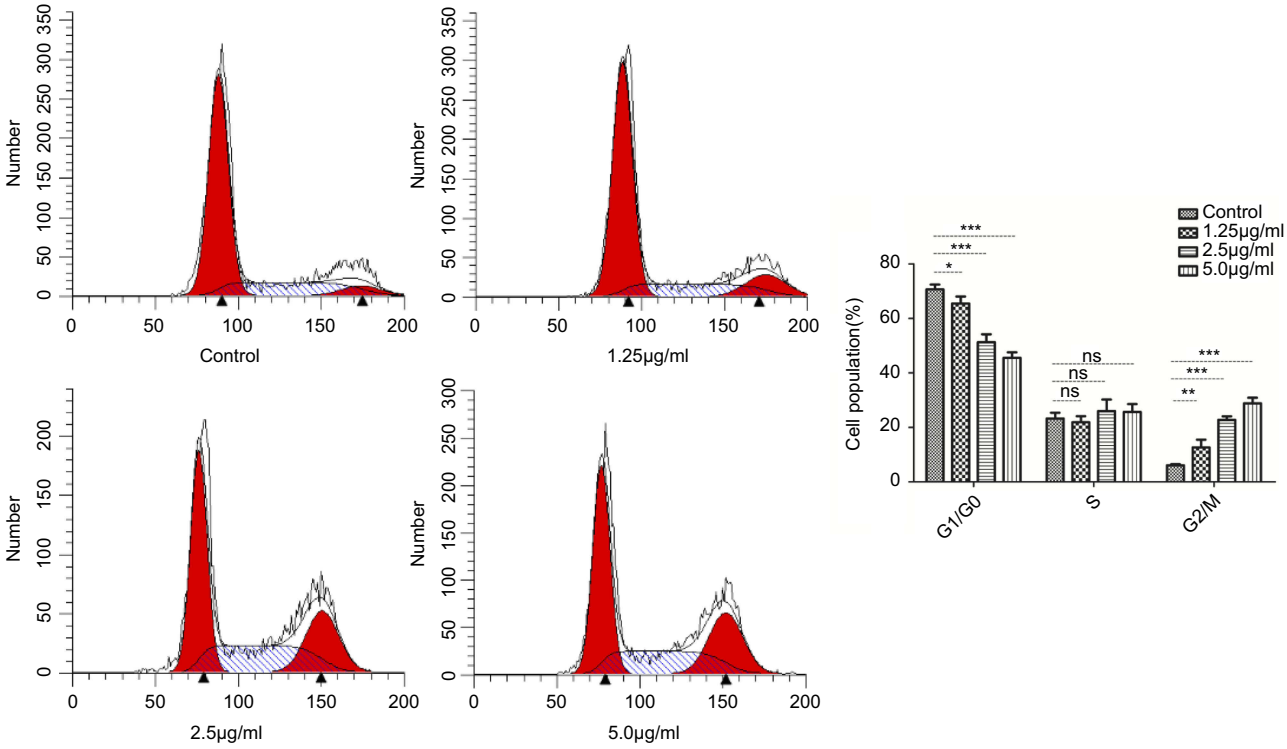

Figure 7 Cell cycle progression assay of HSFs treated with different concentrations of cuprous oxide nanoparticles (CONPs) for 24h. With the increasing concentration of CONPs, the percentage of cells in G2/M phase significantly increased, while the percentage of cells in GO/G1 phase notably decreased, yet the percentage of cells in S phase had no significant change. Column shows the quantitative measurements of the percentage of different cell cycles from three independent experiments. One way ANOVA were used to analyze data (*p<0.05, **p<0.01, ***p<0.001).

of CONPs for 24 h caused significant cell apoptosis in a concentration-dependent manner, especially in the late-stage apoptosis. Both results of flow cytometry analysis and TUNEL staining indicated an evidently increasing apoptosis in HSFs after treated with CONPs in a concentration dependent manner.

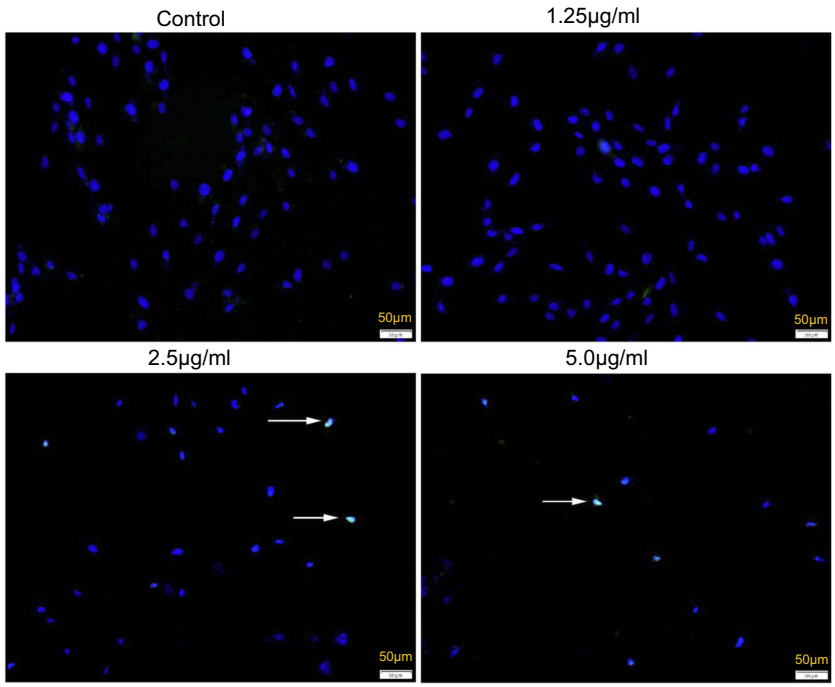

Figure 8 TUNEL assay of apoptosis of HSFs treated with different concentrations of cuprous oxide nanoparticles (CONPs) for 24 h. 2.5 μg/mL and 5.0 μg/mL CONPs caused significant TUNEL positive cells in HSFs.

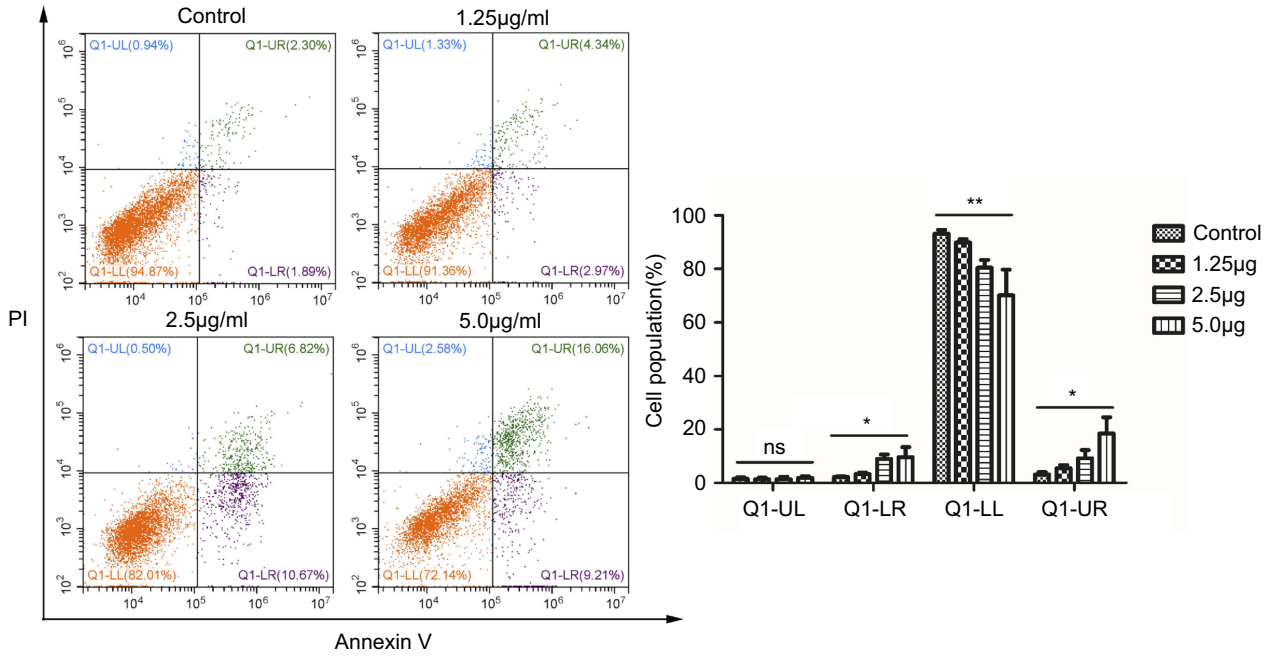

Figure 9 Flow cytometry analysis of HSFs treated with different concentrations of cuprous oxide nanoparticles (CONPs) for 24h, followed by staining with Annexin V-FITC and PI. The apoptosis ratio of HSFs was increased in a dose-dependent manner. Q1-UL, dead cells; Q1-LR, apoptotic cells at the early stage; Q1-LL, live cells; Q1-UR, apoptotic cells at the early stage. The results (mean ± SD) were statistically significant (*p<0.05, **p<0.01), and the assays were performed three times.

CONPs targeted the mitochondria and damaged the mitochondrial membrane potential

Mitochondria is the key structure of energy production, involved in both energy metabolism and free radical metabolism. The change of mitochondrial membrane potential indicated the change of functional status, which could cause cellular damage and serious diseases.[19–21] To detect the mechanism of apoptosis, TEM was used to analyze whether CONPs could cross the cell membrane of HSFs after incubated for 3–4 h in 5ug/ml CONPs. As shown in Figure 10, we discovered that several CONPs crossed the cell membrane (A) and entered the mitochondria (B), and lysosome (C).

JC-1-stained flow cytometry assay was also performed to detect the change of mitochondrial membrane potential (ΔΨm) after treated with CONPs. The results showed that the ratio of the red fluorescent intensity to the green fluorescent intensity gradually decreased with the increasing concentration of CONPs, which indicated a significant drop of mitochondrial membrane potential in a concentration-dependent manner in HSFs treated with CONPs (Figure 11A).

CONPs increased ROS generation in HSFs

Mitochondria was the major source of ROS production in the cells. Increasing intracellular ROS played a very vital role in cell apoptosis. Therefore, we detected whether the endocytosed CONPs in HSFs could increase the production of intracellular ROS. As shown in Figure 11B, we observed that intracellular ROS levels in HSFs

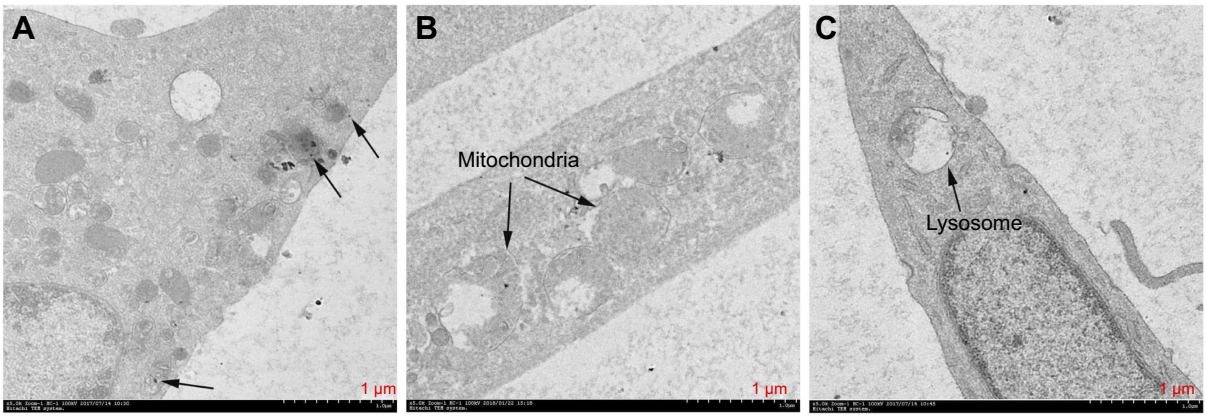

Figure 10 Electron microscopy images showing the ultrastructure of HSFs incubated for 3–4 h in 5 μg/mL cuprous oxide nanoparticles (CONPs). Several CONPs crossed the cell membrane (**A**) and entered the mitochondria (**B**), and lysosome (**C**).

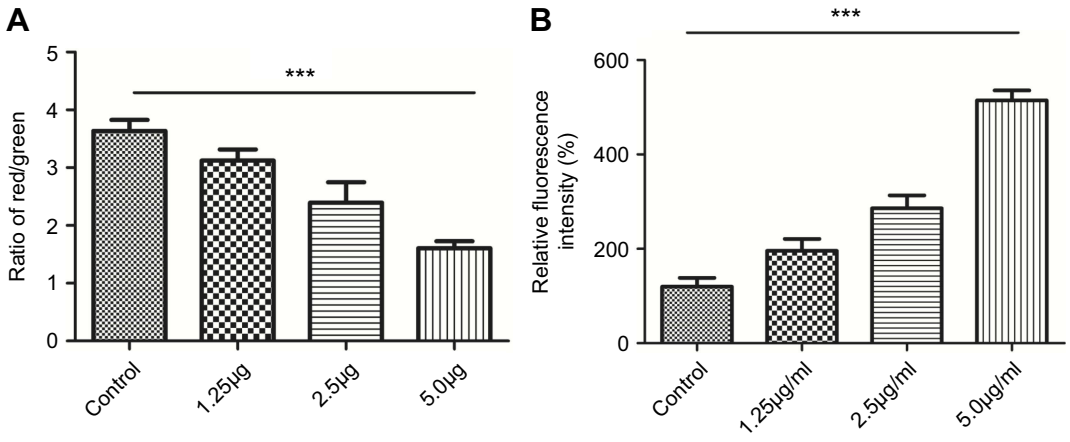

Figure 11 JC-1 (**A**) and ROS (**B**). (**A**) The ratio of the red fluorescent intensity to the green fluorescent intensity gradually decreased with the increasing concentration of cuprous oxide nanoparticles (CONPs); (**B**) intracellular ROS levels in HSFs significantly increased in a concentration-dependent manner after treated with CONPs. The results were statistically significant (***$p<0.001$), and the assays were performed three biological times.

significantly increased in a concentration-dependent manner after treated with CONPs.

Discussion

Although, the specific molecular mechanism of hypertrophic scar formation remain poorly understood, the abnormal biological behavior of HSFs plays a vital role in hypertrophic scar formation and development, such as excessive proliferation, cytokine production, and abnormal accumulation of extracellular matrix (ECM). Previous researches have shown that apoptosis could effectively reduce fibroblasts number, viability, collagen deposition and promote scars mature[22,23] and the mitochondrial priming (proximity to the apoptotic threshold) of myofibroblasts was higher than normal fibroblast.[24] Therefore, inhibiting proliferation by inducting apoptosis in HSFs could be an effective strategy for anti-hypertrophic scar therapy. Recently, nanoparticles have showed great potential in inducing intrinsic and extrinsic apoptotic pathways.[25] CONPs have also showed broad anti-tumor characteristics by inhibiting proliferation and inducing apoptosis in tumor cells.[12–26] The current study, for the first time, revealed the anti-scarring capacity of CONPs by inhibiting proliferation and inducing apoptosis in HSFs in vivo and in vitro.

Previously published studies have shown that apoptosis mainly included the extrinsic pathway (activated by ligand engagement of cell surface death receptors) and the mitochondrial intrinsic pathway.[27] Loss of mitochondrial membrane potential resulted in excessive ROS accumulation which could also impair mitochondrial membranes, leading to the drop of mitochondrial membrane potential.[28,29] Subsequently, the apoptotic factors such as cytochrome c and apoptosis-inducing factor (AIF) were released and the apoptotic cascade and execution of cell death were conducted.[30,31]

In this study, our results suggested that the addition of CONPs could trigger the mitochondrial intrinsic apoptosis in HSFs. The whole process might be shown as follows just as reported in the previous anti-tumor process:[13] The CONPs were first taken up by HSFs in small vesicles, binded to the mitochondrial outer membrane, then released into the mitochondria. Endocytosed CONPs in the mitochondria then impaired the mitochondrial membrane potential, broke the membrane, increased the ROS generation, and finally induced the apoptosis and cell death of HSFs.

The size of nanoparticles is a critical parameter for both efficient cellular uptake and metabolism.[32,33] However, there is still no acknowledged optimum size to maximize the level of cellular uptake. In the current study, CONPs with a mean diameter of 88.5 nm could be uptake and cause the subsequent changes effectively. The low toxicity was also a key characteristic of potential medicine. Nanoparticles of different sizes also possessed different metabolic pathways, smaller than 10 nm through renal clearance,[34] 10−50 nm through the reticuloendothelial system,[35] and larger than 50 nm could only be partially cleared by the liver.[36] Previous study have also showed the low toxicity of CONPs, which could be cleared from the tested organs of the mice quickly,[17] however, the toxicity and biodistribution of CONPs in scars still need to be further explored in the future. The effect of different size nanoparticles on wound healing and anti-scarring also needs to be further studied.

However, there were still some limitations in this study. In the current study, we mainly focused on the therapeutic effects of the CONPs on HSFs. Although TEM, JC-1-stained flow cytometry assay, and ROS detection were conducted to explore the specific apoptosis mechanism, the evidence was still not very enough and convincing. The further mechanism still need to be explored in the future. Angiogenesis also plays an important role during hypertrophic scar formation and inhibiting angiogenesis has been verified to be an effective strategy for anti-hypertrophic scar therapy.[37,38] Though the previous study has revealed that CONPs could effectively inhibit angiogenesis in vitro,[39] the effect of the CONPs on the angiogenesis during the scar formation still need be futher explored.

Conclusion

CONPs showed great therapeutic potential in the treatment of hypertrophic scar by inhibiting fibroblasts proliferation and activating the HSFs apoptosis.

Acknowledgments

This work was funded by the National Natural Science Foundation of China (81701905, 81772076, 81871559, 81372058, 81571897), Shanghai Pujiang Program (17PJD043), "Twelfth Five-Year" Scientific Program of China (AWS14C001, 201502028, AWS11J008), Clinical Key Discipline Project of Shanghai and China, and Shanghai Health System Excellent Talent Training Program (2017BR037).

Disclosure

The authors declare no conflicts of interest in this work.

References

1. Ledon JA, Savas J, Franca K, Chacon A, Nouri K. Intralesional treatment for keloids and hypertrophic scars: a review. *Dermatol Surg*. 2013;39:1745–1757. doi:10.1111/dsu.12346
2. Hardy MA. The biology of scar formation. *Phys Ther*. 1989;69:1014–1024. doi:10.1093/ptj/69.12.1014
3. Zhang J, Li Y, Bai X, Li Y, Shi J, Hu D. Recent advances in hypertrophic scar. *Histol Histopathol*. 2018;33:27–39. doi:10.14670/HH-11-908
4. Niessen FB, Spauwen PH, Schalkwijk J, Kon M. On the nature of hypertrophic scars and keloids: a review. *Plast Reconstr Surg*. 1999;104:1435–1458.
5. Rabello FB, Souza CD, Farina JJ. Update on hypertrophic scar treatment. *Clinics (Sao Paulo)*. 2014;69:565–573. doi:10.6061/clinics/2014(08)11
6. Steinstraesser L, Flak E, Witte B, et al. Pressure garment therapy alone and in combination with silicone for the prevention of hypertrophic scarring: randomized controlled trial with intraindividual comparison. *Plast Reconstr Surg*. 2011;128:306e–313e. doi:10.1097/PRS.0b013e3182268c69
7. Sheridan RL. Burn care: results of technical and organizational progress. *JAMA*. 2003;290:719–722. doi:10.1001/jama.290.6.719
8. Moulin, V., Larochelle S, Langlois C et al. Normal skin wound and hypertrophic scar myofibroblasts have differential responses to apoptotic inductors. *J Cell Physiol*. 2004;198:350–358. doi:10.1002/jcp.10415
9. Zhang J, Liu Z, Cao W, et al. Amentoflavone inhibits angiogenesis of endothelial cells and stimulates apoptosis in hypertrophic scar fibroblasts. *Burns*. 2014;40:922–929. doi:10.1016/j.burns.2013.10.012
10. Shi J, Xiao H, Li J, et al. Wild-type p53-modulated autophagy and autophagic fibroblast apoptosis inhibit hypertrophic scar formation. *Lab Invest. A J Tech Methods and Pathology*. 2018;98(11):1423–1437.
11. Zhou X, Xie Y, Xiao H, et al. MicroRNA-519d inhibits proliferation and induces apoptosis of human hypertrophic scar fibroblasts through targeting Sirtuin 7. *Biomedicine & pharmacotherapy = Biomedicine & Pharmacotherapie*. Apr 2018;100:184–190.
12. Yang Q, Wang Y, Yang Q, et al. Cuprous oxide nanoparticles trigger ER stress-induced apoptosis by regulating copper trafficking and overcoming resistance to sunitinib therapy in renal cancer. *Biomaterials*. 2017;146:72–85. doi:10.1016/j.biomaterials.2017.09.008
13. Hu Y, Wang Y. Cuprous oxide nanoparticles selectively induce apoptosis of tumor cells. *Int J Nanomed*. 2641. 2012;7:2641–52. doi: 10.2147/IJN.S31133.
14. Sankar R, Baskaran A, Shivashangari KS, Ravikumar V. Inhibition of pathogenic bacterial growth on excision wound by green synthesized copper oxide nanoparticles leads to accelerated wound healing activity in Wistar Albino rats. *J Mater Sci Mater Med*. 2015;26:214. doi:10.1007/s10856-015-5543-y
15. Borkow G, Gabbay J, Dardik R, et al. Molecular mechanisms of enhanced wound healing by copper oxide-impregnated dressings. *Wound Repair Regen*. 2010;18:266–275. doi:10.1111/j.1524-475X.2010.00573.x
16. Wang Y, Zi X-Y, Su J, et al. Cuprous oxide nanoparticles selectively induce apoptosis of tumor cells. *Int J Nanomedicine*. 2012;7:2641–2652. doi:10.2147/IJN.S31133
17. Wang Y, Yang F, Zhang H-X, et al. Cuprous oxide nanoparticles inhibit the growth and metastasis of melanoma by targeting mitochondria. *Cell Death Dis*. 2013;4:e783. doi:10.1038/cddis.2013.314
18. Morris DE, Wu L, Zhao LL, et al. Acute and chronic animal models for excessive dermal scarring: quantitative studies. *Plast Reconstr Surg*. 1997;100:674–681.
19. Chan DC. Mitochondria: dynamic organelles in disease, aging, and development. *Cell*. 2006;125:1241–1252. doi:10.1016/j.cell.2006.06.010
20. Duchen MR. Mitochondria in health and disease: perspectives on a new mitochondrial biology. *Mol Aspects Med*. 2004;25:365–451. doi:10.1016/j.mam.2004.03.001
21. Huttemann M, Lee I, Pecinova A, Pecina P, Przyklenk K, Doan JW. Regulation of oxidative phosphorylation, the mitochondrial membrane potential, and their role in human disease. *J Bioenerg Biomembr*. 2008;40:445–456. doi:10.1007/s10863-008-9169-3
22. Rai NK, Tripathi K, Sharma D, Shukla VK. Apoptosis: a basic physiologic process in wound healing. *Int J Low Extrem Wounds*. 2005;4:138–144. doi:10.1177/1534734605280018
23. Desmouliere A, Badid C, Bochaton-Piallat ML, Gabbiani G. Apoptosis during wound healing, fibrocontractive diseases and vascular wall injury. *Int J Biochem Cell Biol*. 1997;29:19–30.
24. Lagares, D., Santos A, Grasberger PE, et al. Targeted apoptosis of myofibroblasts with the BH3 mimetic ABT-263 reverses established fibrosis. *Sci Transl Med*. 2017;9. doi:10.1126/scitranslmed.aal3765
25. Mohammadinejad, R., Moosavi MA, Tavakol S, et al. Necrotic, apoptotic and autophagic cell fates triggered by nanoparticles. *Autophagy*. Jan 2019;15(1):4–33.
26. Wang Y, Yang Q-W, Yang Q, et al. Cuprous oxide nanoparticles inhibit prostate cancer by attenuating the stemness of cancer cells via inhibition of the Wnt signaling pathway. *Int J Nanomedicine*. 2017;12:2569–2579. doi:10.2147/IJN.S130537
27. Campbell KJ, Tait S. Targeting BCL-2 regulated apoptosis in cancer. *Open Biol*. 2018;8. doi:10.1098/rsob.180002
28. Green DR, Reed JC. Mitochondria and apoptosis. *Science*. 1998;281:1309–1312. doi:10.1126/science.281.5381.1309
29. Hockenbery DM, Giedt CD, O'Neill JW, Manion MK, Banker DE. Mitochondria and apoptosis: new therapeutic targets. *Adv Cancer Res*. 2002;85:203–242.
30. Singh KK. Mitochondria damage checkpoint, aging, and cancer. *Ann N Y Acad Sci*. 2006;1067:182–190. doi:10.1196/annals.1354.022
31. Sinha N, Panda PK, Naik PP, et al. Abrus agglutinin promotes irreparable DNA damage by triggering ROS generation followed by ATM-p73 mediated apoptosis in oral squamous cell carcinoma. *Mol Carcinog*. 2017;56:2400–2413. doi:10.1002/mc.22679
32. Mos quera J, Garcia I, Liz-Marzan LM. Cellular uptake of nanoparticles versus small molecules: a matter of size. *Acc Chem Res*. 18 Sep 2018;51(9):2035–2313.
33. Li Z, Tang S, Wang B, et al. Metabolizable small gold nanorods: size-dependent cytotoxicity, cell uptake and in vivo biodistribution. *ACS Biomaterials Science & Engineering*. 2016 2016;2(5):789–797.
34. Zhang X, Luo Z, Chen J, et al. Storage of gold nanoclusters in muscle leads to their biphasic in vivo clearance. *Small*. 2015;11:1683–1690. doi:10.1002/smll.201402233
35. Cho W, Cho M, Jeong J, et al. Acute toxicity and pharmacokinetics of 13 nm-sized PEG-coated gold nanoparticles. *Toxicol Appl Pharmacol*. 2009;236:16–24. doi:10.1016/j.taap.2008.12.023
36. Walkey CD, Olsen JB, Guo H, Emili A, Chan WCW. Nanoparticle size and surface chemistry determine serum protein adsorption and macrophage uptake. *J Am Chem Soc*. 2012;134:2139–2147.
37. Song Y, Yu Z, Song B, et al. Usnic acid inhibits hypertrophic scarring in a rabbit ear model by suppressing scar tissue angiogenesis. *Biomed Pharmacother*. 2018;108:524–530. doi:10.1016/j.biopha.2018.06.176
38. Wang J, Chen H, Shankowsky HA, Scott PG, Tredget EE. Improved scar in postburn patients following interferon-alpha2b treatment is associated with decreased angiogenesis mediated by vascular endothelial cell growth factor. *J Interferon Cytokine Res*. 2008;28:423–434. doi:10.1089/jir.2007.0104
39. Song H, Wang W, Zhao P, Qi Z, Zhao S. Cuprous oxide nanoparticles inhibit angiogenesis via down regulation of VEGFR2 expression. *Nanoscale*. 2014;6:3206. doi:10.1039/c3nr04363k